DYNAMICS OF PARTIALLY INTERACTING COMPOSITE BEAMS

O. A. B. Hassan[1*], S. Grundberg[1], U. A. Girhammar[2]

[1]*Department of Applied Physics and Electronics, Umeå University, SE-90187 Umeå, Sweden*
[2]*Division of Structural and Construction Engineering, Luleå University of Technology, SE-971 87 Luleå, Sweden*

** osama.hassan@tfe.umu.se*

Keywords: Composite beams, interlayer slip, structural vibration, eigenfrequency.

Abstract

The dynamic behaviour of layered composite beams with partial interaction is analysed using variational calculus. The theoretical results are compared with those from dynamic tests on simply supported beams with varying shear connection stiffness between the layers. The influence of the shear connection stiffness on the flexural natural frequencies, flexural deflection and damping is investigated. A good agreement between the analytical and experimental results is obtained.

1 Introduction

Composite or hybrid beams are formed by combining two or more layers or components of like or unlike materials. Such structures are often used in building and bridge construction, and in aircraft and watercraft applications, especially as sandwich constructions. A specific application is vibration of floor structures [1]. The different layers or components are usually attached to each other by means of adhesives or mechanical connectors. Usually, with adhesives, full composite action is achieved, but with mechanical connectors, only partial composite action will develop. The characteristic of the mechanical connectors is usually expressed in terms of slip modulus or shear connection stiffness.

This study is focused on the vibrational behaviour of partially composite beams and determining the natural mode shapes and frequencies, deflection and damping as influenced by the shear connector stiffness.

Vibrations of composite beams with partial interaction have been studied by a few researchers, both analytically and by using finite element methods. Both Euler-Bernoulli and Timoshenko models have been applied. However, corresponding experimental studies are not so frequent in the literature. Some of the early works are that of Henghold [2], who investigated eigenfrequencies and damping of layered beams including slip, and Girhammar and Pan [3]. Later, works of Xu and Wu [4] and Girhammar et al. [5] have been published in this field. Moreover, Wu and Xu [6] included the effect of axial load in their analysis. With respect to sandwich beams, the work of Sainsbury and Zhang [7], Wang and Wereley [8], Bozhevolnaya and Sun [9], and Koutsawa and Daya [10] can for example be mentioned.

This work is part of a research project dealing with the dynamic behaviour of partially composite beams with and without axial loading. The focus is on the experimental evaluation and validation of the theoretical models. The main application is floor vibrations, but also general vibrations in partially interacting layered, laminated, and sandwich-type of structures.

In the dynamic tests, the influence of the shear connection stiffness on the flexural natural frequencies, flexural deformation and damping is investigated.

2 Theory

2.1 Basic assumptions

Consider a composite beam consisting of n layers interacting through shear connectors at the n-1 interlayer interfaces. In the general case, the beam is subjected to a distributed load $q(x)$ along its length L as well as an axial load F, see Fig.1. The individual layer has the elastic modulus E_i, area A_i and the distance z_i from the global coordinate system to the centroid of the individual layer. In a local description, the axial displacement and the Hookean stresses in an individual layer at the point (x,z) at time t is given by

$$u_i(x,z,t) = u_i(x,z_i,t) - \frac{\partial w(x,t)}{\partial x}(z-z_i); \quad z \in A_i \tag{1}$$

$$\sigma_i(x,z,t) = E_i\left[\frac{\partial u_i(x,z_i,t)}{\partial x} - \frac{\partial^2 w(x,t)}{\partial x^2}(z-z_i)\right], \quad z \in A_i \tag{2}$$

where $u_i(x,z_1,t)$ is the axial displacement of the middle line (centroidal line) of the individual layer.

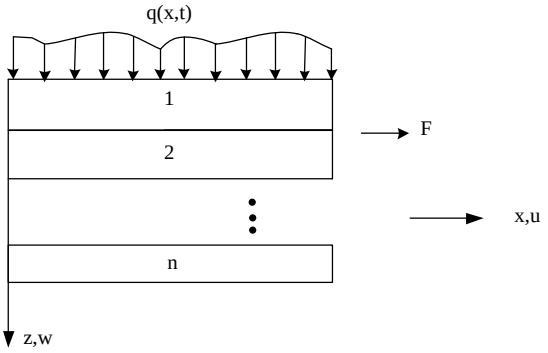

Figure 1. Composite beam consisting of n layers with interlayer slip. The beam is subjected to a distributed load, $q(x,t)$, and an axial force, F.

The slip (Fig. 2a) at the interface i between layers i and i + 1 is according to Eq. (1) given by

$$u_{si} = u_{i+1} - u_i + r_i\frac{\partial w}{\partial x} \tag{3}$$

where $u_i = u_i(x,z_i,t)$ and $u_{i+1} = u_{i+1}(x,z_{i+1},t)$ denote the axial displacements at the centroids of layers i and i+1, respectively, $w(x,t)$ the lateral displacement, and r_i the distance between the centroids of layers i and i + 1. The corresponding interlayer slip force per unit length (V_{si}) can then be written as

$$V_{si} = K_i u_{si}; \quad i = 1,....,n-1 \tag{4}$$

where K_i [N/m^2] is the constant slip modulus for the individual interlayer as is usually assumed in the linear elastic composite action theory. For the solution and applied example according to Section 2.5, it is assumed that $K_i = K$.

2.2 Internal normal forces and moments

A free body diagram of the internal normal forces and moments, shear forces and interlayer slip forces for the individual layers is shown in Fig. 2b. The corresponding forces and moments acting over whole cross-section are also shown in the figure. It is now assumed that the coordinate axis is located in the centroid of the fully composite section and that the axial load is applied along the *x*-axis. This implies that the axial force will induce only axial strain in the composite member and that the total axial force (F) is distributed to the individual layers (F_i) according to their axial stiffnesses, i.e.

$$\sum_{i=1}^{n} F_i = \sum_{i=1}^{n} \frac{E_i A_i}{EA_0} F = F \tag{5}$$

In Fig. 2a, the interlayer slip between two consecutive layers is illustrated (cf. Eq. (3)). This section will be focused on the internal moments and normal forces.

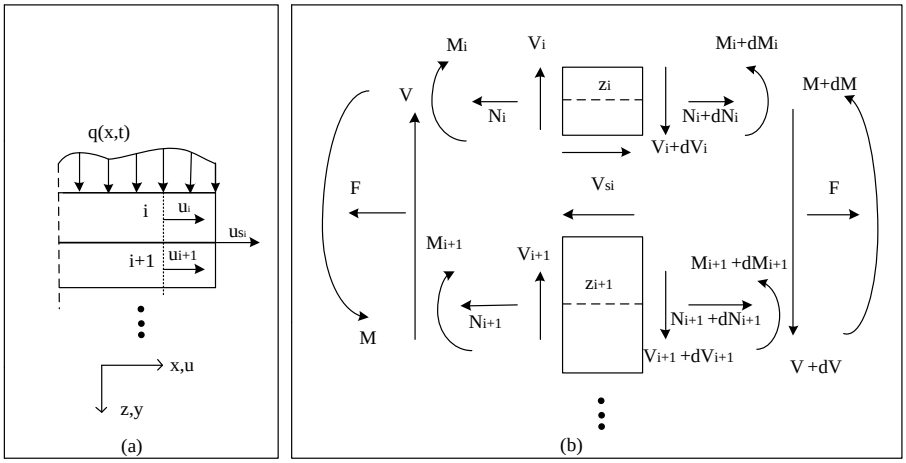

Figure 2. (a) The interlayer slip u_{si} between layers i and i + 1 depends on the axial displacements u_i and u_i+1 of the two layers, respectively; (b) Internal forces and moments acting on each of the n layers together with forces and moments acting on the whole cross-section.

Axial equilibrium gives the total normal force F acting on the whole cross-section at any position x along the beam as

$$F = \sum_{i=1}^{n} (\int_{A_i} \sigma_i \, \mathrm{d}A) = \sum_{i=1}^{n} (E_i \int_{A_i} [\frac{\partial u_i}{\partial x} - \frac{\partial^2 w}{\partial x^2}(z - z_i)] \mathrm{d}A) = \sum_{i=1}^{n} E_i A_i \frac{\partial u_i}{\partial x} = \sum_{i=1}^{n} N_i \tag{6}$$

where Eq. (2) has been used (the term associated with the curvature becomes after the integration), and N_i is the axial force on the cross section along the centroidal axis of the individual layer. Moment equilibrium gives the total moment M acting on the whole cross section of the beam at a location x as

$$\begin{aligned} M &= \sum_{i=1}^{n} (\int_{A_i} (z - z_i)\sigma_i \, \mathrm{d}A) = \sum_{i=1}^{n} \{E_i \int_{A_i} [-(z - z_i)^2 \frac{\partial^2 w}{\partial x^2} + z_i (z - z_i) \frac{\partial u_i}{\partial x}] \mathrm{d}A\} \\ &= \sum_{i=1}^{n} \{-E_i I_i \frac{\partial^2 w}{\partial x^2} + z_i E_i A_i \frac{\partial u_i}{\partial x}\} = \sum_{i=1}^{n} (M_i + z_i N_i) \end{aligned} \tag{7}$$

2.3 Potential and kinetic energy

Expressions for the associated potential energy from the action of the internal normal forces and moments, and slip forces are needed in the derivation of the equations of motion from Hamilton's principle. Shear forces will be neglected as in the Euler-Bernoulli's model. The potential energy associated with the axial and bending normal stresses can be expressed as

$$\begin{aligned} U_{\text{layers}} &= \sum_{i=1}^{n}\left(\frac{1}{2}\int_{V_i}\sigma_i\varepsilon_i\,\mathrm{d}V\right) = \frac{1}{2}\sum_{i=1}^{n}\left\{\int_0^L\left\{\int_{A_i}E_i\left(\frac{\partial u_i}{\partial x}-(z-z_i)\frac{\partial^2 w}{\partial x^2}\right)^2\mathrm{d}A\right\}\mathrm{d}x\right. \\ &= \left.\frac{1}{2}\sum_{i=1}^{n}\left\{\int_0^L\left\{\int_{A_i}\left[E_i\left(\frac{\partial u_i}{\partial x}\right)^2 - E_i(z-z_i)^2\left(\frac{\partial^2 w}{\partial x^2}\right)^2\right]\mathrm{d}A\right\}\mathrm{d}x = U_a + U_b\right. \end{aligned} \tag{8}$$

where the potential energy associated with uniform axial strain of the both layers are given by

$$U_a = \frac{1}{2}\sum_{i=1}^{n}\left\{\int_0^L E_i A_i\left(\frac{\partial u_i}{\partial x}\right)^2\mathrm{d}x\right\} \tag{9}$$

and the potential energy associated with bending is

$$U_b = \frac{1}{2}\sum_{i=1}^{n}\left\{\int_0^L E_i I_i\left(\frac{\partial^2 w}{\partial x^2}\right)^2\mathrm{d}x\right\} = \frac{1}{2}\int_0^L EI_0\left(\frac{\partial^2 w}{\partial x^2}\right)^2\mathrm{d}x \quad ; \quad EI_0 = \sum_{i=1}^{n}E_i I_i \tag{10}$$

where I_i is the moments of inertia of the individual layer. The potential energy stored in the interlayer connectors is given by

$$U_s = \frac{1}{2}\sum_{i=1}^{n-1}\int_0^L K_i\,u_{si}^2\,\mathrm{d}x \tag{11}$$

The kinetic energy of the system is given by

$$T = \frac{1}{2}\int_0^L\left[\left(\sum_{i=1}^{n-1}m_i\right)\left(\frac{\partial w}{\partial t}\right)^2\right]\mathrm{d}x\,; \quad m = \sum_{i=1}^{n}m_i \tag{12}$$

where m_i is the mass per unit length of the individual layer.

2.4 External loadings

External loadings give rise to work or potential energy. The composite beam will here be considered subjected to general loads as distributed transversal load $q(x, t)$ and an axial load F. External boundary loads and masses are discussed separately. The distributed load produces the following work due to the deflection and the axial load due to the axial displacement of the ends as a consequence of the deflection

$$W_q = \int_0^L q(x,t)\,w(x,t)\,\mathrm{d}x\,; \quad W_F = -\frac{1}{2}F\int_0^L\left(\frac{\partial w}{\partial x}\right)^2\mathrm{d}x \tag{13}$$

2.5 Boundary loadings and masses

The composite beam will here be considered subjected to both time-independent boundary loadings as axial loads, end moments and end shear-type of forces, and time-dependent boundary conditions as concentrated end masses. Including concentrated masses at the ends in the analytical models is a way to take test fittings into account when evaluating the test results. The boundary loadings and masses and their corresponding work or energy expressions can be included in the Lagrangian function in the variational analysis or directly be included in the expressions for the total shear force and bending moment at the respective end of the beam [5]. In this paper, the latter approach is adopted.

At the end $x = x_B = [0, L]$, the total bending moment M_{B,x_B} and the total shear force V_{B,x_B} are included directly in the boundary conditions for the moment and shear force or as the sum of their individual boundary moments and shear forces, respectively, as

$$M_{B,x_B} = \sum_{i=1}^{n} \int_{A_i} (z - z_i)\sigma_{i,B,x_B} \, \mathrm{d}A\big|_{x=x_B} ; \quad V_{B,x_B} = \sum_{i=1}^{n} \int_{A_i} \tau_{i,B,x_B} \, \mathrm{d}A\big|_{x=x_B} ; \quad F_i = \frac{E_i A_i}{EA_0} F \tag{14}$$

where σ_{i,B,x_B} and τ_{i,B,x_B} are expressions for the normal and shear stresses on the end cross-section of the individual layer. However, for the axial load, the third equation in Eq. (14), the individual axial force F_i needs to be used.

According to d'Alembert's principle, concentrated masses give rise to shear forces and moments. Here we will neglect the rotary inertia, i.e. we will neglect the moment effect of the masses. The shear force effect of the masses can be expressed as

$$V_{m_{B,x_B}} = \pm m_{B,x_B} \left. \frac{\partial^2 w}{\partial t^2} \right|_{x=x_B} \tag{15}$$

where m_{B,x_B} is the concentrated mass at the end $x_B = [0, L]$, and the upper sign refers to $x_B = 0$ and the lower to $x_B = L$.

2.5 Dynamic response of partially composite beams – Application to three-layer beams

Using variational calculus with respect to the potential and kinetic energies according to Eqs. (9) - (13), the following governing differential equation for the deflection is obtained

$$\frac{\partial^6 w}{\partial x^6} - (\alpha^2 + \frac{F}{EI_0}) \frac{\partial^4 w}{\partial x^4} + \frac{\alpha^2 F}{EI_\infty} \frac{\partial^2 w}{\partial x^2} - \frac{1}{EI_0} \frac{\partial^2 q}{\partial x^2} + \frac{\alpha^2 q}{EI_\infty} = \frac{\alpha^2 m}{EI_\infty} \frac{\partial^2 w}{\partial t^2} - \frac{m}{EI_0} \frac{\partial^4 w}{\partial x^2 \partial t^2} \tag{16}$$

where α and β shear connector parameters, and EI_∞ and EI_0 the bending stiffness of the fully and non-composite section, respectively.

Applied to a composite beam with three equal layers as the test specimen according to Fig. 3, the internal normal force and the different parameters are given by

$$N_1 - F_1 = \frac{EI_\infty}{\alpha^2 r} \left[-\frac{\partial^4 w}{\partial x^4} + \alpha^2 \left((1 - \frac{EI_0}{EI_\infty}) + \frac{F}{\alpha^2 EI_0} \right) \frac{\partial^2 w}{\partial x^2} - \frac{m}{EI_0} \frac{\partial^2 w}{\partial t^2} + \frac{q}{EI_0} \right] \tag{17}$$

$$\alpha^2 = K[\frac{1}{EA} + \frac{r^2}{2EI_0}]; \quad \beta = \frac{Kr}{2EI_0}; \quad EI_\infty = EI_0[1 + \frac{EAr^2}{2EI_0}]; \quad EI_0 = \sum_{i=1}^{3} E_i I_i \tag{18}$$

where N_1 (= – N_3) is the force in the outer layer (N_2 = 0 due to symmetry), r is the distance between the centroids of the outer layers (i = 1 and i = 3).

2.6 Application to simply supported three-layer composite beams without axial load
The test specimens (Fig. 3) are simply supported composite beams with three equal layers and with no axial load (F = 0). Using the boundary conditions: $w = \partial^2 w/\partial x^2 = \partial^4 w/\partial x^4 = 0$ at x = 0, L, the solution of Eq. (16) yields the following expression for the circular eigenfrequencies

$$\omega_n^2 = \omega_{\infty,n}^2 \left\{ 1 - \left[1 + \frac{1 + (\frac{\alpha}{k_{1,n}})^2}{\frac{EI_\infty}{EI_0} - 1} \right]^{-1} \right\}, \qquad \omega_{\infty,n}^2 = \frac{EI_\infty k_{1,n}^4}{m} \tag{19}$$

where k_n is the wave number ($k_n = n\pi/L$), and $\omega_{\infty,n}$ the eigenfrequencies of a fully composite beam. For equal layers of width b and height h, the following parameters are obtained

$$\alpha^2 = \frac{9K}{Ebh} \quad ; \quad EA_0 = 3Ebh \quad ; \quad EI_0 = E\frac{bh^3}{4} \quad ; \quad EI_\infty = 9EI_0 \tag{20}$$

The slip modulus K or the shear connection stiffness αL is evaluated by conducting a static deflection test. The maximum static deflection ($w_{\max}$) for a simply supported beam subjected to a mid-point load is given by [11]

$$\frac{w_{\max} - w_{\infty,\max}}{w_{\infty,\max}} = \frac{24}{(\alpha L)^3}(\frac{EI_\infty}{EI_0} - 1)(\frac{\alpha L}{2} - \tanh\frac{\alpha L}{2}) \tag{21}$$

where $w_{\infty,\max}$ is the maximum deflection for a fully composite beam.

3 Method and equipment

The experiments were performed on a composite beam consisting of three layers of aluminium (E = 70 GPa; ρ = 2700 kg/m^3) having a length of 2 m and a rectangular cross section of width 80 mm and height 5 mm. The aluminium layers were connected by maximally 19 pairs of plugs of the material polyoxymethylene (POM) with a diameter of 8 mm, see Fig. 3. The parameters for the beam became as follows: EI_0 = 175 Nm^2, EI_∞ = 1575 Nm^2, m = 3.24 kg/m, k_1 = 1.57 m^{-1}, and $f_{\infty,1}$ = 8.65 Hz. The acceleration of the beam was measured by a capacitive accelerometer (LIS3L06AL MEMS inertial sensor) from ST Microelectronics connected to a signal conditioning device. The accelerometer has a frequency range from DC up to 1.5 kHz. The accelerometer signal conditioning device is connected to a laptop computer running the software Audacity® for storing the recorded signal in wave-format. The dimensionless shear connection stiffness, αL, which includes the slip modulus according to Eq. (18), of the partial interaction of the beam is determined from measurement of the steady state deflection of the beam under a static load at mid-span (Eq. (21)). The deflection is measured using a dial gauge. The vibration experiments are first performed on a beam connected by 19 × 2 = 38 plugs and then again on the same beam with half of the plugs dismantled. The accelerometer is mounted at mid-span of the beam in order

to detect the fundamental mode of the beam. The vibrations of the beam are excited by a gentle manual push and the oscillations are then recorded during a time interval lasting around 40 s.

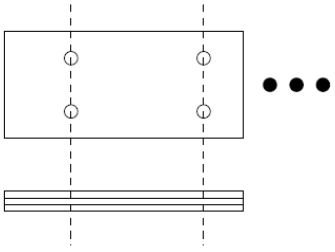

Figure 3. The composite beam consisted of three layers of aluminium connected by plugs of the material POM (polyoxymethylene). The individual layers had a width of 80 mm and height 5 mm. The overall length of the beam is 2 m. There are 19 pairs of plugs at a distance of 10 cm.

4 Results

The measurements were performed on beams connected by 38 and 19 POM plugs as shear connectors, respectively. For 38 plugs the measured fundamental frequency was 8.7 Hz; the corresponding power spectrum is presented in Fig. 4 (right curve). The measured damping was 0.28 s^{-1} and the modal damping ratio was 0.0051. For the static test on the composite beam loaded the deflection at mid-span was measured. This yielded a shear connection stiffness of $\alpha L = 23$ and the effective bending stiffness was calculate to give $EI_{\text{eff}} = 1.4$ kNm^2. For 19 plugs the measured fundamental frequency was 8.1 Hz; the corresponding power spectrum is shown in Fig. 4 (left curve). The damping was 0.16 s^{-1} and the modal damping ratio was 0.0031. The deflection measurement yielded, $\alpha L = 13$ and $EI_{\text{eff}} = 1.1$ kNm^2.

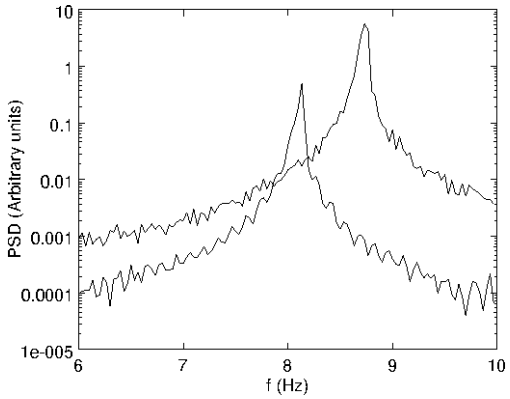

Figure 4. Acceleration power spectrum density for the composite beam connected by 19 plugs (maximum to the left) and 38 plugs (maximum to the right), respectively.

A summary of results for both cases is presented in Table 1.

Case	EI_{eff} (kNm^2)	αL	f_{theory} (Hz)	f_{exp} (Hz)	ζ
1(38 plugs)	1.4	23	8.5	8.7	0.0051
2 (19 plugs)	1.1	13	7.5	8.1	0.0031

Table 1. Results for the composite beam with 38 plugs and 19 plugs, respectively; αL is the shear connection stiffness, EI_{eff} the effective bending stiffness, f_{theory} the theoretical fundamental eigenfrequency, f_{exp} the measured eigenfrequency, and ζ the modal damping ratio of the fundamental mode.

5 Discussion

The measured shear connection stiffness, αL = 23, for the case when all the 38 plugs were inserted into the beam, indicates that the partial interaction of this beam was so strong that it behaved almost like a fully composite beam. In the second case, when 19 plugs were used as connectors between the layers, the deflection experiments yielded αL = 13, which implies that a weaker partial interaction is produced in this case.

The damping of the structural vibrations is caused by: (1) dissipation in the plastic plugs connecting the layers; (2) friction between the layers; and (3) friction at the boundaries. The fact that the damping was lower in the second case (19 plugs) suggests that the damping is mainly due to energy dissipation in the plugs.

Acknowledgement

The authors wish to express their sincere appreciation for the financial support from The European Union's Structural Funds – The Regional Fund.

References

[1] Hassan O.A.B. *Building acoustics and vibration*: *theory and practice*. World scientific publications, Singapore (2009).

[2] Henghold W.M. *Layered beam vibrations including slip*. Doctoral Dissertation, Colorado State University (1972).

[3] Girhammar U.A., Pan D.H. Exact static analysis of partially composite beams and beam-columns. *International Journal of Mechanical Sciences*, **49**, pp. 239–255 (2007).

[4] Xu R.,Wu Y. Static, dynamic, and buckling analysis of partial interaction composite members using Timoshenko's beam theory. *International Journal of Mechanical Sciences* 2007;49:1139–55.

[5] Girhammar U.A., Pan D.H., Gustafsson A. Exact dynamic analysis of composite beams with partial interaction. *International Journal of Mechanical Sciences*, 51, pp. 565–582 (2009).

[6] Wu Y-F., Xu R., Chen W. Free vibrations of the partial-interaction composite members with axial force. *Journal of Sound and Vibration* 2006; 299(4–5):1074–93.

[7] Sainsbury M.G., Zhang Q.J. The Galerkin element method applied to the vibration of damped sandwich beams. *Computers and Structures* 1999;71:239–56.

[8] Wang G., Wereley N.M. Spectral finite element analysis of sandwich beams with passive constraint layer damping. *Journal of Vibration and Acoustics* 2002;124:376–86.

[9] Bozhevolnaya E., Sun J.Q. Free vibration analysis of curved sandwich beams. *Journal of Sandwich Structures and Materials* 2004;6:47–72.

[10] Koutsawa K., Daya E.M. Static and free vibration analysis of laminated glass beam on viscoelastic supports. *International Journal of Solids and Structures* 2007;44:8735–50.

[11] Girhammar U.A., Pan D.H. Exact static analysis of partially composite beams and beam-columns. *International Journal of Mechanical Sciences*, 51, pp. 565–582 (2009).